Highly Efficient Red-Electrophosphorescent Devices Based on Polyfluorene Copolymers Containing Charge-Transporting Pendant Units

Fang-Iy Wu, Ping-I Shih, Ya-Hsien Tseng, Guan-Yu Chen, Chen-Han Chien, and Ching-Fong Shu*

Department of Applied Chemistry, National Chiao Tung University, 300 Hsinchu, Taiwan

Yung-Liang Tung and Yun Chi*

Department of Chemistry, National Tsing Hua University, 300 Hsinchu, Taiwan

Alex K.-Y. Jen

Department of Materials Science and Engineering, Box 352120, University of Washington, Seattle, Washington 98195-2120

Received: April 5, 2005; In Final Form: May 26, 2005

We have systematically examined the photoluminescence (PL) and electroluminescence (EL) behavior of blends comprising two efficient red phosphors doped, respectively, into the blue-emitting polyfluorene derivatives **PF-TPA-OXD** and **PF-OXD**. The host polymers, which contain both hole- and electron-transporting or merely electron-transporting side chains, are capable of facilitating charge injection and transport. After determining the HOMO and LUMO energy levels of these materials, we were able to match the dopant with its most suitable host to achieve the direct formation and confinement of an exciton at the dopant. This configuration also leads to a reduction in the electrical excitation of the host polymer, which in turn decreases the degree of exciton loss arising from nonradiative decay of the host triplet. Using this approach, we were able to realize the production of high-performance red-electrophosphorescent devices. For **Os(fppz)**-doped devices, we obtain a balanced charge recombination in conjunction with higher current and luminance when using **PF-TPA-OXD** as the host matrix; this device reached a maximum external quantum efficiency of 8.37% with a peak brightness of 16 720 cd/m^2. The absence of charge-transporting pendant units, i.e., the device fabricated from poly[9,9-dioctylfluorene-2,7-diyl] (**POF**), led, however, to relatively poor electroluminescence characteristics (5.81% and 2144 cd/m^2).

Introduction

Organic light-emitting diodes (OLEDs) have been the subject of a great number of investigations because of their potential applications in flat-panel displays. During the electrical operation of OLEDs, the holes and electrons that are injected from opposite electrodes combine together to form singlet (S) and triplet (T) excitons. In a typical fluorescent OLED system, only the radiative decay of the singlet excitons is effective; that of the triplet excitons is inhibited by the rule of spin conservation and is, therefore, very inefficient.[1] Recently, highly efficient electrophosphorescent OLEDs have been demonstrated through the use of heavy-metal phosphors as the light-emitting media.[2−7] The strong spin−orbit coupling induced by the heavy metal promotes S−T intersystem crossing and enhances the subsequent T_1-S_0 transition. EL devices based on these phosphors allow both singlet and triplet excitons to be harvested; theoretically, the internal efficiency can reach as high as 100%.[8]

Electrophosphorescent LEDs whose host materials are polymers are attractive because they can be processed at room temperature and they have the potential to allow large-area devices to be fabricated using low-cost and simple manufacturing techniques, such as spin-casting or inkjet printing at room temperature. Efficient devices based on electrophosphorescent polymers have been achieved through the doping of polymers, such as **POF** and poly(vinylcarbazole) (PVK), with Pt,[9−11] Ir,[5−7,12−20] Os,[21,22] Re,[23] Ru,[24] and Cu[25] complexes. In the doped devices, two kinds of emission mechanisms are possible. One involves excitation transfer from the host to the organometallic emitter (through Forster and/or Dexter energy transfer mechanisms), and the other involves direct recombination of the injected charges on the dopant site, i.e., a charge-trapping mechanism.[26−28] For the purpose of balancing charges, some electron-transporting materials, such as 2-(4-biphenylyl)-5-(4-*tert*-butylphenyl)-1,3,4-oxadiazole (PBD) and 3-(4-biphenylyl)-4-phenyl-5-(4-*tert*-butylphenyl)-1,2,4-triazole (TAZ), have also been introduced to compensate for the poor ability of the host polymers to transport electrons.[15−17,29] In addition, codoping with the hole-transporting molecule *N*,*N*′-diphenyl-*N*,*N*′-(bis-(3-methylphenyl)-[1,1-biphenyl]4,4′-diamine) (TPD)[18] can decrease the driving voltage, which results in a further improvement in the device's power efficiency. Physical blending of these charge-transporting molecules into polymeric hosts does, however, increase the risk of phase separation at higher loadings.

Ir complex-doped devices, formed using a host matrix of polyfluorene homopolymer presenting charge-transporting units at its termini, exhibit higher device efficiency because of their improved charge-injection and -transport ability.[30] Unfortunately, the introduction of charge-transporting moieties as terminal

* Authors to whom correspondence should be addressed. E-mail: shu@cc.nctu.edu.tw (C.F.S.).

10.1021/jp051747k CCC: $30.25
Published on Web 07/06/2005

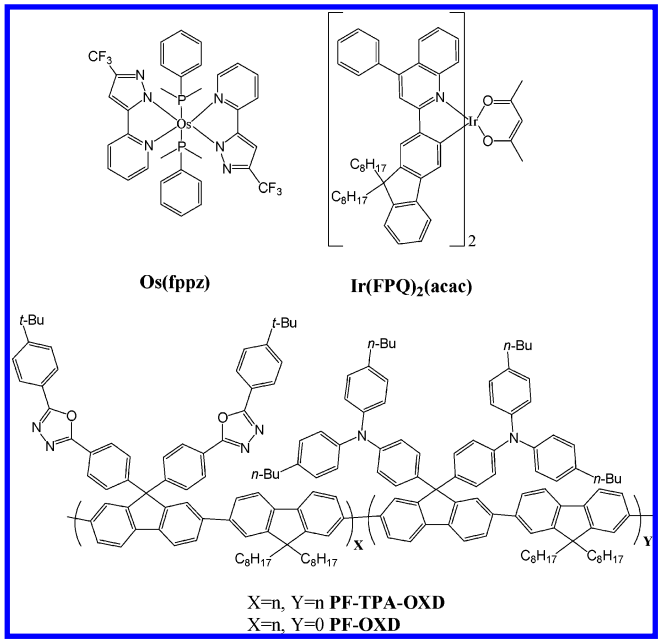

Figure 1. Chemical structures of **Os(fppz)**, **Ir(FPQ)$_2$(acac)**, **PF-TPA-OXD**, and **PF-OXD**.

groups limits their loading amounts in the resulting polymers to only a few percent, which would be far below the optimal value required to obtain a good charge balance.[17] In a previous study, we found that **PF-OXD**,[31] a fluorene-based copolymer possessing two electron-transporting groups (**OXD**s) in alternating fluorene units, exhibited good spectrum stability with high efficiency upon either optical or electrical excitation. Subsequently, we achieved a more-balanced charge recombination in electroluminescent devices by synthesizing **PF-TPA-OXD**,[32] another fluorene-based copolymer possessing both hole- and electron-transporting moieties as side chains. These two blue fluorene-based copolymers are very promising candidates as host materials in molecular-doped electrophosphorescence devices because of their wide energy gaps and large numbers of charge-transporting pendant groups, which provide for improved confinement of the triplet excitons in the phosphorescent dopants and efficient charge transportation, respectively.[33,34] In addition, **PF-OXD** and **PF-TPA-OXD** exhibit high glass transition temperatures (T_g) at 213 and 166 °C, respectively, which we attribute to the presence of the rigid pendant groups.[31,32] Such high values of T_g, which prevent morphological change and suppress the formation of aggregates upon exposure to heat, are desirable for polymers that are used as emissive materials for light-emitting applications. Furthermore, UV−vis absorption spectra reveal that, in the ground state, the polyfluorene main chain and the charge-transporting pendant groups preserve their individual absorption characteristics, i.e., there is no interaction between them. Photoluminescence studies indicate that efficient energy transfer occurs from the photoexcited pendant groups to the polymer backbone; this process may contribute significantly to the emission intensity of the main chain.[31,32]

In this article, we describe our systematic investigation of the photoluminescence (PL) and electroluminescence (EL) behavior of blends of **PF-TPA-OXD** or **PF-OXD**, as a blue-emitting conjugated host, doped with the efficient red phosphors **Os(fppz)**[35] and **Ir(FPQ)$_2$(acac)**.[20] Figure 1 displays the chemical structures of these red dopants and polymeric hosts. The built-in charge-transporting groups are connected to the backbones of the **PF-TPA-OXD** and **PF-OXD** polymers through the sp^3-hybridized carbon atoms of their fluorene unit, (this approach does not disturb the optical properties[31,32] of the backbone) such that the total number of charge-transporting moieties is equal to the number of fluorene units in the backbone. If we know their energy levels [i.e., the highest-occupied molecular orbital (HOMO) and the lowest-unoccupied molecular orbital (LUMO)], we can match the host with its most suitable dopant to achieve the direct formation and confinement of the exciton at the dopant. For devices having the general structure ITO/PEDOT/polymers/TPBI/MgAg, efficient red LEDs having a maximum external quantum efficiency of ca. 8.5% and a brightness above 16 000 cd/m^2 can be realized if the direct recombination of the injected charges on the dopants is the main operating mechanism for exciton production.

Experimental Section

Materials. The syntheses of **Os(fppz)**[35] and **Ir(FPQ)$_2$(acac)**[20] have been published elsewhere. The polymeric hosts[31,32] **PF-TPA-OXD**, **PF-OXD**, and **POF** were synthesized through Suzuki coupling polymerization, as reported previously. The electron-transporting material, 1,3,5-tris(*N*-phenylbenzimidazol-2-yl)benzene (TPBI),[36] was prepared according to reported procedures; it was sublimated twice prior to use.

Characterization. UV−Vis spectra were recorded using an HP 8453 diode-array spectrophotometer. Photoluminescence (PL) spectra were obtained on a Hitachi F-4500 luminescence spectrometer. Cyclic voltammetry (CV) measurements were performed using a BAS 100 B/W electrochemical analyzer. The oxidation and reduction potentials were measured, respectively, in anhydrous CH_2Cl_2 and anhydrous THF, containing 0.1 M $TBAPF_6$ as the supporting electrolyte, at a scan rate of 50 mV s^{-1}. The potentials were measured against an Ag/Ag$^+$ (0.01 M $AgNO_3$) reference electrode using ferrocene as the internal standard. The onset potentials were determined from the intersection of two tangents drawn at the rising current and background current of the cyclic voltammogram.

Farbrication of Light-Emitting Devices. We fabricated LED devices having the general structure ITO/poly(styrenesulfonate)-doped poly(3,4-ethylenedioxythiophene) (PEDOT) (35 nm)/polymer emitting layer (50−70 nm)/TPBI (30 nm)/Mg:Ag (100 nm)/Ag (100 nm). The PEDOT was spin-coated directly onto the ITO glass and dried at 80 °C for 12 h under vacuum to improve hole injection and the substrate's smoothness. The emitting layer, a polyfluorene derivative doped with red phosphor in different molar ratios (from 0.3 to 1.5 mol %, corresponding to phosphor/fluorene unit ratios of the polyfluorene backbone from 0.3:100 to 1.5:100), was then spin-cast onto the surface of the PEDOT and dried for 3 h at 60 °C under vacuum. Prior to film casting, the polymer solution was filtered through a Teflon filter (0.45 μm). The TPBI layer, which we used as an electron transporting layer that would also block holes and confine excitons, was grown by thermal sublimation in a vacuum of 3×10^{-6} Torr.[37] Subsequently, the cathode, Mg:Ag (10:1, 100 nm) alloy, was deposited by coevaporation onto the TPBI layer; this process was followed by placing an additional layer of Ag (100 nm) onto the alloy as a protection layer. The current−voltage luminance relationships were measured under ambient conditions using a Keithley 2400 source meter and a Newport 1835C optical meter equipped with an 818ST silicon photodiode.

Results and Discussion

Figure 2 displays the absorption spectra of **Os(fppz)** and **Ir(FPQ)$_2$(acac)**; they overlap well with the host emission of **PF-TPA-OXD** at 400−550 nm. This overlap should enable

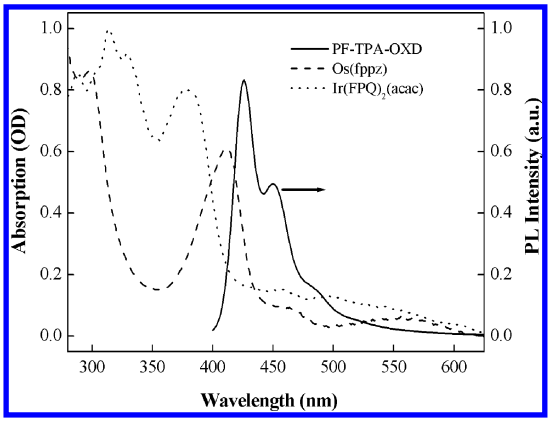

Figure 2. Absorption spectra of **Os(fppz)** and **Ir(FPQ)$_2$(acac)** in dilute solution and the emission spectrum of **PF-TPA-OXD** in the solid state.

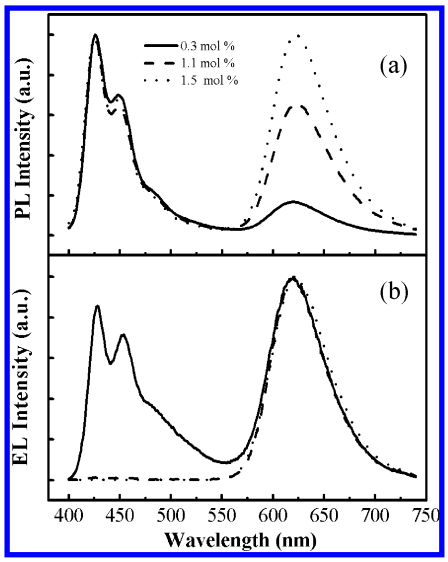

Figure 3. (a) PL and (b) EL spectra of blends prepared from **PF-TPA-OXD** doped with different amounts of **Os(fppz)**.

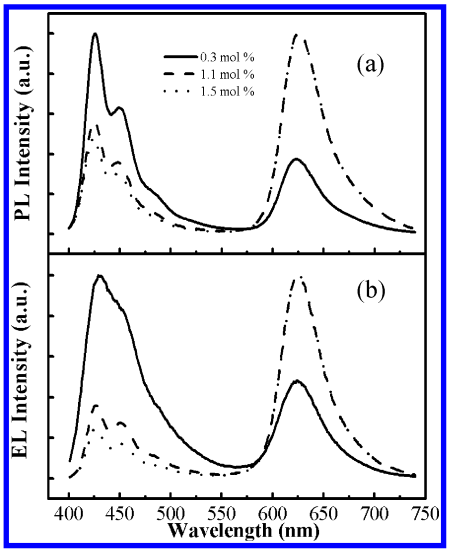

Figure 4. (a) PL and (b) EL spectra of blends prepared from **PF-TPA-OXD** doped with different amounts of **Ir(FPQ)$_2$(acac)**.

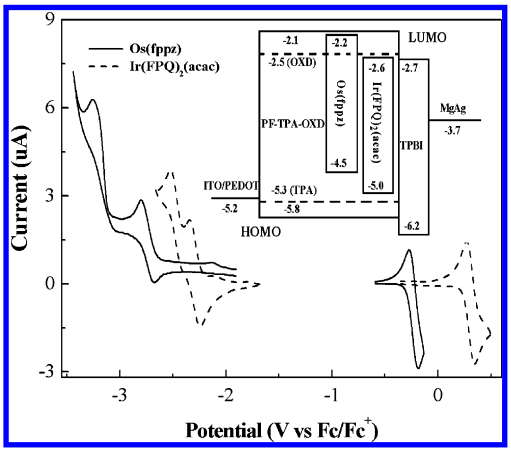

Figure 5. Cyclic voltammograms of **Os(fppz)** and **Ir(FPQ)$_2$(acac)**. The inset displays the proposed energy level scheme for the devices having the configuration ITO/PEDOT/red dopant:**PF-TAP−OXD**/TPBI/MgAg.

efficient Förster energy transfer to occur from the singlet excited state of the polymer host to the metal-to-ligand charge transfer (MLCT) state of the guest, followed by fast intersystem crossing to the triplet state of the dopants and, consequently, radiative decay from its triplet state. The observed exciton lifetimes of **Os(fppz)** and **Ir(FPQ)$_2$(acac)** are 0.7 and 1.3 μs, respectively, which are considerably shorter than that of Ir(btp)$_2$(acac) (5.8 μs).[38] These shorter lifetimes, which may suppress both TT and PT annihilations,[14,39] lead to improved device quantum efficiency, even at a high current density, and result in these complexes being attractive candidates for emitting dopants in electrophosphorescent devices.

Figure 3a presents the degree of energy transfer that occurs between the **PF-TPA-OXD** host and **Os(fppz)** as dopant at doping ratios from 0.3 to 1.5 mol % upon photoexcitation of the host. The PL profiles of the blends contain two components: one, which occurs at ca. 425 nm, is a characteristic emission of polyfluorene from the **PF-TPA-OXD** host, while the other, at ca. 620 nm, corresponds to the triplet emission of **Os(fppz)**. Even at a high doping concentration (1.5 mol %), the PL displays a significant contribution from the **PF-TPA-OXD** host. In contrast, the corresponding EL spectra (Figure 3b) indicate that, at a doping concentration of 1.1 mol %, the dopant emission dominates completely and results in a saturated red triplet emission from the Os complex. The dramatic difference between the PL and EL spectra reveals that Förster energy transfer of an exciton between the host and dopant does not account solely for this observed EL. Another possible mechanism for exciting **Os(fppz)** would be direct charge trapping at the dopant sites followed by recombination with opposite charges.[33,40,41] On the other hand, the PL and EL spectra of the blends of **Ir(FPQ)$_2$(acac)** in **PF-TPA-OXD** as host are quite similar in shape and position for each doping concentration (Figure 4); this observation indicates that energy transfer would remain as the main operating mechanism in the EL process.[41]

To understand the details of the charge-transport mechanism in the blends, we must obtain information regarding the HOMO and LUMO energy levels of these two phosphorescent dopants. To do so, we investigated (Figure 5) their electrochemical behavior using cyclic voltammetry (CV), with ferrocene as the internal standard,[42] and estimated the values of the energy levels from their onset potentials. Both complexes dissolved in CH_2Cl_2 exhibited reversible oxidation during anodic sweeps. These oxidation processes are generally considered to involve predominantly the metal centers[20] and, accordingly, the formal potential for oxidation is very strongly dependent on the oxidation state of the metal atoms [Os(+2) and Ir(+3), respectively]. During the cathodic scan in THF, we observed that a reversible reduction process occurred initially for each complex, followed by a second reductive wave, which was

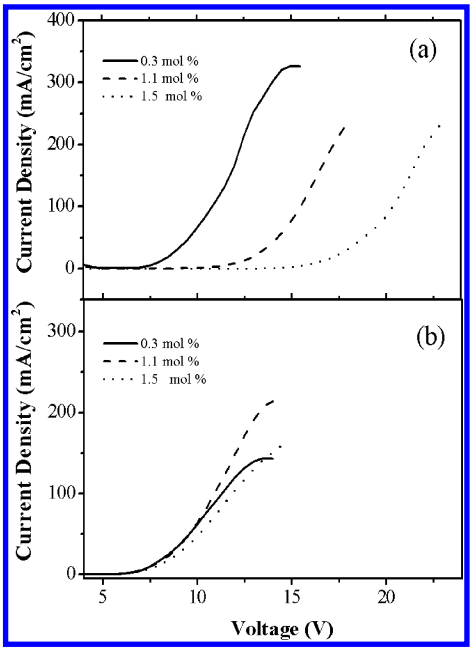

Figure 6. Current density vs voltage characteristics of (a) the **Os(fppz)**-doped and (b) **Ir(FPQ)$_2$(acac)**-doped devices incorporating **PF-TPA-OXD** as host at different doping concentrations.

reversible for the Ir complex and irreversible for the Os complex, at more-negative potential. We assigned the reduction waves of **Os(fppz)** and **Ir(FPQ)$_2$(acac)** primarily to the reduction of their respective fppz and FPQ ligands.[20] On the basis of the onset potentials of the oxidations and reductions, we estimated (see the inset of Figure 5) the HOMO and LUMO energy levels of the complexes with regard to the energy level of ferrocene (4.8 eV below vacuum).[42] These two red-emitting dopants have similar band gaps (ca. 2.3 eV), but different HOMO and LUMO energy levels, which shift to less-negative values (by ca. 0.5 eV) upon proceeding from **Ir(FPQ)$_2$(acac)** (−2.6 and −5.0 eV, respectively) to **Os(fppz)** (−2.2 and −4.5 eV, respectively).

According to the energy level diagram, the HOMO level of **PF-TPA-OXD** occurs at −5.3 eV[32] (corresponding to the TPA side chains). For devices having the configuration ITO/PEDOT/polymers/TPBI/MgAg, holes can easily be injected from PEDOT (−5.2 eV)[43] into the HOMOs of the **TPA** moieties (−5.3 eV) of the **PF-TPA-OXD** host upon overcoming a small energy barrier (0.1 eV). In the case of the **Os(fppz)**-doped devices, the ionization potential of **Os(fppz)** is 0.8 eV below the HOMO level of **PF-TPA-OXD**; therefore, holes can potentially be trapped at **Os(fppz)**, followed by recombination of opposite charges (electrons) to form excitons. As indicated in Figure 6, the plots of current density vs voltage ($I-V$) shift to higher voltages upon increasing the doping concentration of **Os(fppz)** in the **PF-TPA-OXD** host. This result is consistent with the charge-trapping mechanism proposed previously from the observation of a dramatic difference between the PL and EL spectra.[33,40,41] In contrast, the operating voltage for the **Ir(FPQ)$_2$(acac)**-doped devices undergoes no apparent change upon varying the doping concentration from 0.3 to 1.5 mol % (Figure 6b). This situation is the consequence of only a shallow trap (depth of 0.3 eV) constructed by **Ir(FPQ)$_2$(acac)** in the **PF-TPA-OXD** host.[27] Once the holes are trapped at the HOMO of **Ir(FPQ)$_2$(acac)**, there is a high possibility that they may detrap and hop back to the HOMOs of the **TPA** moieties by conquering this smaller energy barrier, and thus, the excitons eventually form again at the host.[44] Thus, most of excitons still form at the host under the influence of the electric field and

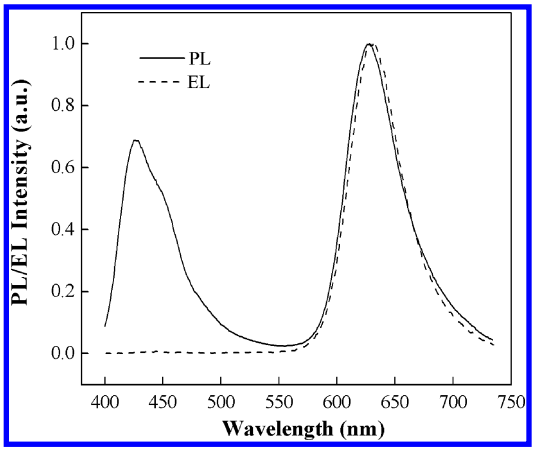

Figure 7. PL and EL spectra of blends prepared from **PF-OXD** doped with **Ir(FPQ)$_2$(acac)** at a doping concentration of 1.0 mol %.

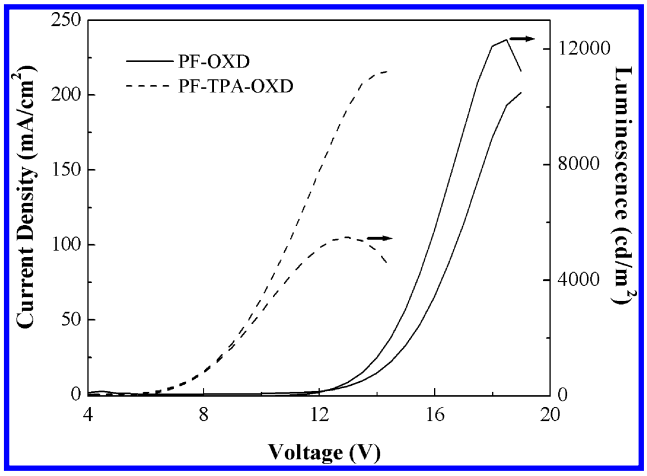

Figure 8. Current density and brightness vs voltage characteristics of **Ir(FPQ)$_2$(acac)**-doped devices incorporating **PF-TPA-OXD** and **PF-OXD** as hosts at a doping of ca. 1 mol %.

then energy transfer to the dopant provides a similar contribution to the triplet emission part as we observed in the PL spectra.

On the basis of the discussion above, **Ir(FPQ)$_2$(acac)** will become a more-effective trap site for holes if **PF-OXD** is employed as the host because the HOMO of **PF-OXD** occurs at −5.8 eV[31] (corresponding to the polyfluorene backbone), which will result in a trap for holes that has a barrier of 0.8 eV. The PL spectrum of the blends prepared from 1.0 mol % **Ir(FPQ)$_2$(acac)** in **PF-OXD** is similar to that of the blend comprising 1.1 mol % **Ir(FPQ)$_2$(acac)** in **PF-TPA-OXD** (see Figure 4a), but it is very different from its EL spectrum, in which the triplet emission is completely dominant (Figure 7). In addition, the plot of the current density vs voltage is clearly shifted to a higher voltage than that of the device incorporating **PF-TPA-OXD** as the host (Figure 8). The increase in operating voltage provides further evidence for holes being trapped by **Ir(FPQ)$_2$(acac)**. Because the trapping of holes in the **Ir(FPQ)$_2$(acac)** sites will build up a positive space-charge field in the host matrix, the further injection of holes from the anode will be impeded, resulting in higher operating voltages.[11,27,45] Furthermore, the exciton formed directly at **Ir(FPQ)$_2$(acac)** can reduce the electrical excitation of the host polymer,[33,44] which may result in exciton loss from the nonradiative decay of the host triplet. Therefore, the maximum external quantum efficiency can be improved from 4.81 to 8.66%, accompanied by an increase in maximum brightness from 5488 cd/m^2 to 12 324 cd/m^2, when **Ir(FPQ)$_2$(acac)** is doped into **PF-OXD** rather than into **PF-TPA-OXD**.

TABLE 1: Performance of Devices Having the Structure ITO/PEDOT/Polymer Emitting Layer/TPBI/Mg:Ag

	Os(fppz)[a]			Ir(FPQ)$_2$(acac)[a]	
	PF-TPA-OXD[b]	PF−OXD[b]	POF[b]	PF-TPA-OXD[b]	PF−OXD[b]
turn-on voltage (V)[c]	7.7	7.6	11.0	4.2	9.8
voltage (V)[d]	13.0 (15.5)	13.2 (16.1)	15.7 (20.8)	8.3 (10.9)	14.4 (16.7)
brightness (cd/m^2)[d]	2342 (9999)	2217 (8622)	1345 (1839)	1022 (4045)	1838 (8228)
luminance efficiency (cd/A)[d]	11.71 (10.00)	11.10 (8.65)	6.75 (1.85)	5.12 (4.05)	9.18 (8.25)
external quantum efficiency (%)[d]	8.36 (7.15)	8.34 (6.49)	5.27 (1.44)	4.75 (3.76)	8.63 (7.76)
maximum brightness (cd/m^2)	16720 (at 18 V)	11548 (at 17.5 V)	2144 (at 19 V)	5488 (at 13 V)	12324 (at 18.5 V)
maximum luminance efficiency (cd/A)	11.72	11.19	7.44	5.18	9.12
maximum external quantum efficiency (%)	8.37	8.41	5.81	4.81	8.66
EL maximum (nm)[e]	620	624	622	624	630
CIE coordinates, x and y[e]	0.65 and 0.34	0.64 and 0.34	0.63 and 0.33	0.48 and 0.23	0.67 and 0.32

[a] Dopant (ca. 1 mol %) [b] Host. [c] Recorded at 1 cd/m^2. [d] Recorded at 20 mA/cm^2 and the data in parentheses were recorded at 100 mA/cm^2. [e] Recorded at 13 V.

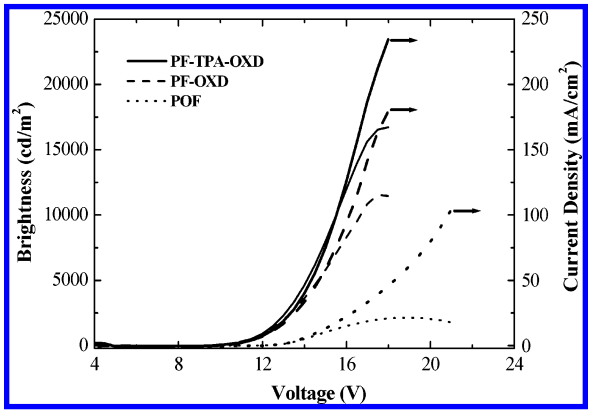

Figure 9. Luminance and current density vs voltage characteristics of **Os(fppz)**-doped devices incorporating **PF-TPA-OXD**, **PF-OXD**, and **POF** as hosts at doping concentrations of 1.1 mol %.

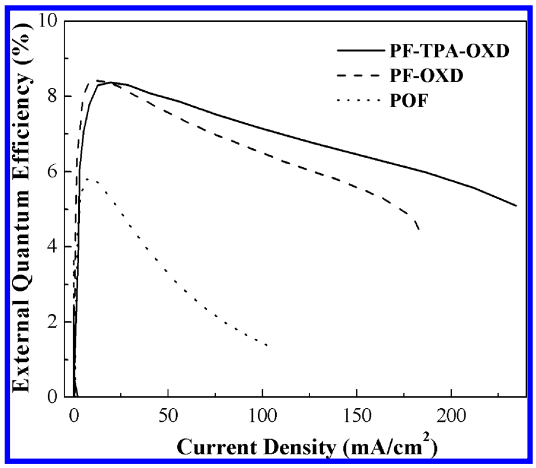

Figure 10. Plot of external quantum efficiency vs current density for **Os(fppz)**-doped devices incorporating **PF-TPA-OXD**, **PF-OXD**, and **POF** as hosts at doping concentrations of 1.1 mol %.

In contrast to the results we obtained for the **Ir(FPQ)$_2$(acac)**-doped devices, there was neither significant difference in the $I-V$ characteristics nor a great improvement in performance of the **Os(fppz)**-doped device when using **PF-OXD** as the host to replace **PF-TPA-OXD** at the same doping concentration (Figures 9 and 10). Furthermore, in comparison with **POF**, we found that the polyfluorene copolymers **PF-TPA-OXD** and **PF-OXD**, which contain charge-transporting groups, do indeed have greater charge-transport abilities. To achieve the same current density, the device incorporating **POF** as the polymeric host obviously requires a higher applied voltage than do the other two. This situation occurs as a result of the positive charge

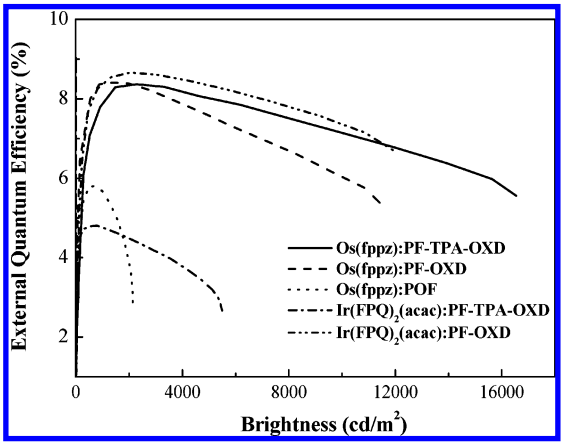

Figure 11. Plot of external quantum efficiency vs luminance of the blends prepared using ca. 1 mol % of dopants.

accumulated within the **POF** blend being unable to effectively recombine with electrons throughout the whole bias range. With the auxiliary **OXD** pendant units attached (i.e., using **PF-TPA-OXD** or **PF-OXD** as the host), more-efficient electron injection and transport can be achieved, which will not only increase the possibility of charge recombination at the trapped holes but also reduce the created positive field.[17] Thus, utilizing **PF-TPA-OXD** or **PF-OXD** as the host in a **Os(fppz)**-doped device can lead to a larger current and a higher device efficiency than those obtained when employing **POF** as the host material. It is worth mentioning that the current density of the device based on the **PF-TPA-OXD** blend is larger than that based on **PF-OXD**. This finding suggests that the incorporation of **TPA** moieties can further improve charge (hole) injection and transport, which will lead to EL devices having higher brightnesses.[18]

Table 1 summarizes the performances of the complex-doped devices at a doping ratio of ca. 1 mol %. Among them, the blend of **Os(fppz)** doped into the **PF-TPA-OXD** host provides the maximum brightness (16 720 cd/m^2), with Commission Internationale de L'Eclairage (CIE) color coordinates of (0.65, 0.34), at 13 V. Apart from the devices comprising 1.1 mol % **Ir(FPQ)$_2$(acac)** in **PF-TPA-OXD** and 1.1 mol % **Os(fppz)** in **POF**, all of the other three devices based on copolymer hosts can maintain more than 70% of their maximum values of quantum efficiency at a luminance above 10^4 cd/m^2 in the region of pure-red emission (Figure 11).

Conclusion

We have realized the preparation of highly efficient red-electrophosphorescent devices incorporating Ir or Os complexes

at low doping contents by using blue polyfluorene copolymers as hosts that contain both hole- and electron-transporting or merely electron-transporting side chains. For the **Ir(FPQ)$_2$(acac)**-doped devices, we obtained a more efficient and saturated red emission that arose through a charge-trapping mechanism that quenched host emission completely when we used **PF-OXD** as the host. Because of its high-lying HOMO levels, **Os(fppz)** can serve as an effective trap site for holes; hence, we obtained efficient devices using both **PF-OXD** and **PF-TPA-OXD** as polymeric hosts. We attribute these high performances to effective exciton confinement within the emitting layer by the hole/exciton blocking layer and successful formation of excitons directly at the dopants; balanced charge recombination reduces electrical excitation of the host polymer and decreases exciton loss through nonradiative decay of the host triplet.

Acknowledgment. We thank the National Science Council for financial support. Our special thanks go to Professor C.-H. Cheng, Dr. J.-P. Duan, and Dr. H.-T. Shih for their support and cooperation during the preparation and characterization of the light-emitting devices.

References and Notes

(1) Klessinger, M.; Michl, J. *Excited States and Photochemistry of Organic Molecules*; VCH: New York, 1995.

(2) Baldo, M. A.; Lamansky, S.; Burrows, P. E.; Thomson, M. E.; Forrest, S. R. *Appl. Phys. Lett.* **1999**, *75*, 4.

(3) Adachi, C.; Baldo, M. A.; Forrest, S. R.; Lamansky, S.; A.; Thompson, M. E.; Kwong, R. C. *Appl. Phys. Lett.* **2001**, *78*, 1622.

(4) Mcgehee, M. D.; Bergstedt, T.; Zhang, C.; Saab, A. P.; O'Regan, M. B.; Bazan, G. C.; Srdanov, V. I.; Heeger, A. J. *Adv. Mater.* **1999**, *11*, 1349.

(5) Lee, C. L.; Lee, K. B.; Kim, J. J. *Appl. Phys. Lett.* **2000**, *77*, 2280.

(6) Yang, M.-J.; Tsutsui, T. *Jpn. J. Appl. Phys.* **2000**, *39*, L828.

(7) Gong, X.; Robinson, M. R.; Ostrowski, J. C.; Moses, D.; Bazan, G. C.; Heeger, A. J. *Adv. Mater.* **2002**, *14*, 581.

(8) Adachi, C.; Baldo, M. A.; Thompson, M. E.; Forrest, S. R. *J. Appl. Phys.* **2001**, *90*, 5048.

(9) Guo, T.-F.; Chang, S.-C.; Yang, Y.; Kwing, R. C.; Thompson, M. E. *Org. Electron.* **2000**, *1*, 15.

(10) Chang, S.-C.; He, G.; Chen, F.-C.; Guo, T.-F.; Yang, Y. *Appl. Phys. Lett.* **2001**, *79*, 2088.

(11) O'Brien, D. F.; Giebler, C.; Fletcher, R. B.; Cadlby, A. J.; Palilis, L. C.; Lidzey, D. C.; Lane, P. A.; Bradley, D. D. C.; Blau, W. *Synth. Met.* **2001**, *116*, 379.

(12) Zhu, W.; Mo, Y.; Yuan, M.; Yang, W.; Cao, Y. *Appl. Phys. Lett.* **2002**, *80*, 2045.

(13) Gong, X.; Ostrowski, J. C.; Bazan, G. C.; Moses, D. *Appl. Phys. Lett.* **2002**, *81*, 3711.

(14) Chen, F.-C.; Yang, Y.; Thompson, M. E.; Kido, J. *Appl. Phys. Lett.* **2002**, *80*, 2308.

(15) Vaeth, K. M.; Tang, C. W. *J. Appl. Phys.* **2002**, *92*, 3447.

(16) Jiang, C.; Yang, W.; Peng, J.; Xiao, S.; Cao, Y. *Adv. Mater.* **2004**, *16*, 537.

(17) Yang, X.; Neher, D.; Hertel, D.; Däubler, T. K. *Adv. Mater.* **2004**, *16*, 161.

(18) Yang, X. H.; Neher, D. *Appl. Phys. Lett.* **2004**, *84*, 2476.

(19) Niu, Y.-H.; Chen, B.; Liu, S.; Yip, H.; Bardecker, J.; Jen, A. K.-Y.; Kavitha, J.; Chi, Y.; Shu, C.-F.; Tseng, Y.-H.; Chien, C.-H. *Appl. Phys. Lett.* **2004**, *85*, 1619.

(20) Wu, F.-I.; Su, H.-J.; Shu, C.-F.; Luo, L.; Diau, W.-G.; Cheng, C.-H.; Duan, J.-P.; Lee, G.-H. *J. Mater. Chem.* **2005**, *15*, 1305.

(21) Kim, J. H.; Liu, M. S.; Jen, A. K.-Y.; Carison, B.; Dalton, L. R.; Shu, C.-F.; Dodda, R. *Appl. Phys. Lett.* **2003**, *83*, 776.

(22) Su, H.-J.; Wu, F.-I.; Shu, C.-F.; Tung, Y.-L.; Chi, Y.; Lee, G.-H. *J. Polym. Sci., Part A: Polym. Chem.* **2005**, *43*, 859.

(23) Kan, S.; Liu, X.; Shen, F.; Zhang, J.; Ma, Y.; Zhang, G.; Wang, Y.; Shen, J. *Adv. Funct. Mater.* **2003**, *13*, 603.

(24) Xia, H.; Zhang, C.; Liu, X.; Qiu, S.; Lu, P.; Shen, F.; Zhang, J.; Ma, Y. *J. Phys. Chem. B* **2004**, *108*, 3185.

(25) Zhang, Q.; Zhou, Q.; Cheng, Y.; Wang, L.; Ma, D.; Jing, X.; Wang, F. *Adv. Mater.* **2004**, *16*, 432.

(26) Lane, P. A.; Palilis, L. C.; O'Brien, D. F.; Giebeler, C.; Cadby, A. J.; Lidzey, D. G.; Campbell, A. J.; Blau, W.; Bradley, D. D. C. *Phys. Rev. B* **2001**, *63*, 235206.

(27) Yang, X. H.; Neher, D.; Scherf, U.; Bagnich, S. A.; Bässler, H. *J. Appl. Phys.* **2003**, *93*, 4413.

(28) Gong, X.; Ostrowski, J. C.; Moses, D.; Bazan, G. C.; Heeger, A. J. *Adv. Funct. Mater.* **2003**, *13*, 439.

(29) Tokito, S.; Suzuki, M.; Sato, F.; Kamachi, M.; Shirane, K. *Org. Electron.* **2003**, *4*, 105.

(30) Gong, X.; Ma, W.; Ostrowski, J. C.; Bechgaard, K.; Bazan, G. C.; Heeger, A. J.; Xiao, S.; Moses, D. *Adv. Funct. Mater.* **2004**, *14*, 393.

(31) Wu, F.-I.; Reddy, D. S.; Shu, C.-F.; Liu, M. S.; Jen, A. K.-Y. *Chem. Mater.* **2003**, *15*, 269.

(32) Shu, C.-F.; Dodda, R.; Wu, F.-I.; Liu, M. S.; Jen, A. K.-Y. *Macromolecules* **2003**, *36*, 6698.

(33) Chen, F.-C.; Chang, S. C.; He, G.; Pyo, S.; Yang, Y.; Kurotaki, M.; Kido, J. *J. Polym. Sci., Part B: Polym. Phys.* **2003**, *41*, 2681.

(34) Chen, F.-C.; He, G.; Yang, Y. *Appl. Phys. Lett.* **2003**, *82*, 1006.

(35) Tung, Y.-L.; Wu, P.-C.; Liu, C.-S.; Chi, Y.; Yu, J.-K.; Hu, Y.-H.; Chou, P.-T.; Peng, S.-M.; Lee, G.-H.; Tao, Y.; Carty, A. J.; Shu, C.-F.; Wu, F.-I. *Organometallics* **2004**, *23*, 3745.

(36) Shi, J.; Tang, C. W.; Chen, C. H. U.S. Patent 5,645,948, 1997.

(37) Culligan, S. W.; Geng, Y.; Chen, S. H.; Klubek, K.; Vaeth, K. M.; Tang, C. W. *Adv. Mater.* **2003**, *15*, 1176.

(38) Lamansky, S.; Djurovich, P.; Murphy, D.; Abdel-Razzaq, F.; Lee, H.-E.; Adachi, C.; Burrows, P. E.; Forrest, S. R.; Thompson, M. E. *J. Am. Chem. Soc.* **2001**, *123*, 4304.

(39) Baldo, M. A.; Adachi C.; Forrest, S. R. *Phys. Rev. B* **2000**, *62*, 10967.

(40) Noh, Y.-Y.; Lee, C.-L.; Kim, J.-J.; Yase, K. *J. Chem. Phys.* **2003**, *118*, 2853.

(41) Uchida, M.; Adachi, C.; Koyama, T.; Taniguchi, Y. *J. Appl. Phys.* **1999**, *86*, 1680.

(42) Pommerehne, J.; Vestweber, H.; Guss, W.; Mahrt, R. F.; Bässler, H.; Porsch, M.; Daub, J. *Adv. Mater.* **1995**, *7*, 551.

(43) Brown, T. M.; Kim, J. S.; Friend, R. H.; Cacialli, F.; Daik, R.; Feast, W. J. *Appl. Phys. Lett.* **1999**, *75*, 1679.

(44) Cleave, V.; Yahiglu, G.; Barny, P. L.; Hwang, D.-H.; Holmes, A. B.; Friend, R. H.; Tessler, N. *Adv. Mater.* **2001**, *13*, 44.

(45) Virgili, T.; Lidzey, D. C.; Bradley, D. D. C. *Synth. Met.* **2000**, *111*, 203.